ACS Photonics

pubs.acs.org/journal/apchd5

Letter

Visible Wavelength Flatband in a Gallium Phosphide Metasurface

Christopher Munley, Arnab Manna, David Sharp, Minho Choi, Hao A. Nguyen, Brandi M. Cossairt, Mo Li, Arthur W. Barnard, and Arka Majumdar*

Cite This: https://doi.org/10.1021/acsphotonics.3c00175

Read Online

ACCESS | Metrics & More | Article Recommendations | Supporting Information

ABSTRACT: Engineering the dispersion of light in a metasurface allows for controlling the light−matter interaction strength between light confined in the metasurface and materials placed within its near-field. Specifically, engineering a flatband dispersion increases the photonic density of states, thereby enhancing the light−matter interaction. Here, we experimentally demonstrate a metasurface with a flat dispersion at visible wavelengths. We designed and fabricated a suspended one-dimensional gallium phosphide metasurface and measured the photonic band structure via energy-momentum spectroscopy, observing a photonic band that is flat over 10° of half angle at ∼590 nm. We integrated cadmium selenide nanoplatelets with the metasurface and measured coupled photoluminescence into the flatband. Our demonstration of a photonic flatband enables the possibility of integrating emerging quantum emitters to the metasurface with possible applications in nonlinear image processing and topological photonics.

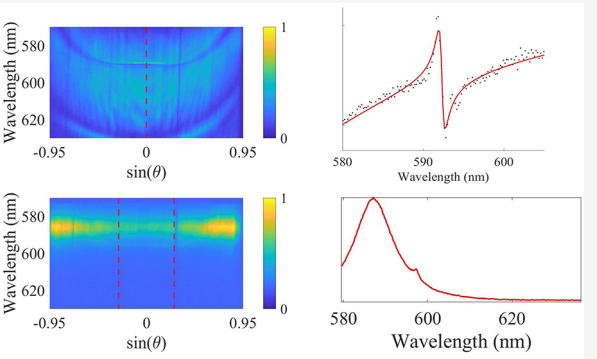

KEYWORDS: *metasurfaces, nanoparticles, flatbands, optical properties*

INTRODUCTION

The ability to engineer band-topology via subwavelength patterning has opened up new opportunities in nanophotonic structures, including metasurfaces. Among various band-topologies, photonic flatbands are of particular importance, as the photonic density of states increases near the flatband, with potential applications in enhancing nonlinear interactions between photons and creation of "slow light". Photonic flatbands have already been experimentally realized in diverse systems, including arrays of waveguides and coupled cavity arrays.[1−4] Metasurfaces have also been employed to realize flatband dispersion in an ultracompact geometry, but most of them have very poor out-coupling to the free-space mode, and thus are not suitable to access via free-space excitation.[5] Photonic flatbands accessible via free space excitation have primarily been limited to terahertz and infrared metasurfaces.[6,7] With many emerging quantum emitters in visible wavelengths, a photonic flatband in this wavelength regime opens up opportunities to study interaction with a greater diversity of emitters. However, realizing a visible flatband metasurface is challenging due to the necessity of a material with a high refractive index and fabrication complexity coming from very small geometric features.

Here we designed and fabricated a flatband metasurface at ∼590 nm using gallium phosphide (GaP). The choice of GaP is motivated by its high index ($n \approx 3.4$ at the wavelength of interest) and negligible loss across visible wavelengths.[8] In fact, GaP photonic structures have already been used to enhance emission from atomically thin 2D materials and solution processed quantum materials.[9,10] Here, a commercially available chemical vapor deposited GaP thin film on silicon was partially etched to break the vertical symmetry and then released from the silicon to create a suspended metasurface. We probed the flatband in reflection via energy-momentum spectroscopy, demonstrating a band which is flat over 10° of half angle with a measured quality factor estimated to be 750, corresponding to a line width of ∼0.5 nm. Finally, we integrated cadmium selenide (CdSe) nanoplatelets (NPLs) on top of the GaP metasurface and demonstrated flat-band-coupled photoluminescence (PL).

DEVICE DESIGN

We designed the flatband metasurface using rigorous coupled wave analysis (RCWA) in an S4 package[11] integrated with Lumerical's finite-difference time-domain (FDTD) simulation. Our design utilizes vertical symmetry breaking in a dimerized high contrast grating to control band topology while maintaining a mode with a long lifetime (see Figure 1a).[12] The vertical symmetry of the metasurface is broken via partial etching of the GaP film. This couples the even and odd modes

Received: February 6, 2023

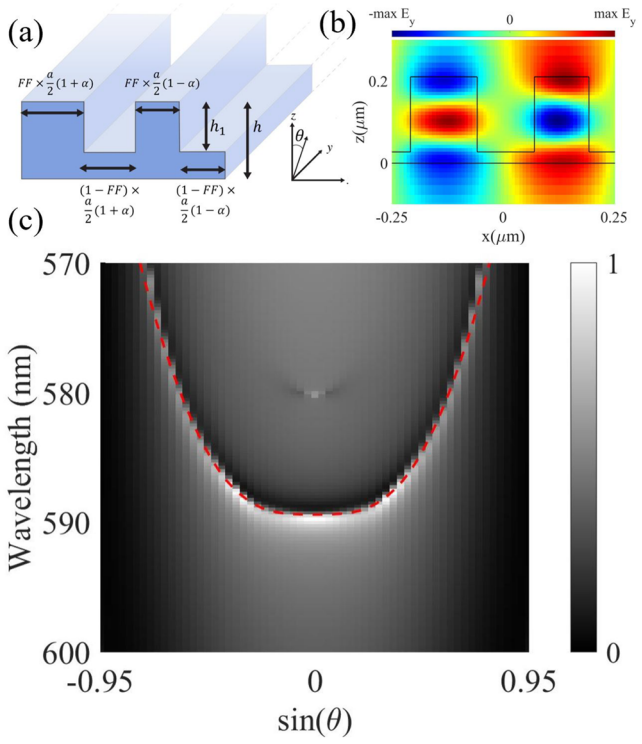

Figure 1. (a) Schematic of the cross-section of the metasurface showing the period of the metasurface a, period-doubling perturbation α, the percentage of the lattice filled with dielectric, called the fill factor FF, and the total and partially etched heights (h and h_1, respectively). We measure the in-plane dispersion as the angle of reflection varies along the $y-z$ plane, perpendicular to the direction of periodicity. (b) Simulated y-direction electric field of one period of the metasurface at the resonance of the flatband with normally incident light. (c) Simulated photonic band structure shows a flat band near 590 nm. The red-dashed line indicates the resonant wavelength determined at each angle by fitting with a Fano resonance.

of the periodic grating, and a flatband is realized through the interference of these even and odd modes.[13] Additionally, the periodicity of the grating is perturbed by a period-doubling asymmetry, α, allowing for efficient free space coupling to bands.[14] While the period, a, determines the wavelength of resonance, the fill factor, FF, and the partial etching depth, h_1, control the dispersion of the band. All of these parameters are free, but all fabricated metasurfaces on the same chip will share the same etch depth, while lateral free parameters like fill factor and period can vary from device to device. We note that the designed flatband in this paper is due to the fine-tuning of parameters, and thus should be considered an "accidental" flatband, as defined by Leykam et al.[15] Hence, the flat dispersion can be destroyed by any fabrication imperfection, as opposed to topological flatbands that retain band dispersion in the presence of fabrication disorder due to the symmetry of their sublattices. To overcome this sensitivity to fabrication, we fabricated an array of devices, altering the fill factor and period for each device, ensuring that even in the presence of over- and underetching of the partial etch depth due to inherent uncertainty in fabrication, we would be able to find a device with the designed photonic flatband. In our device, a 210 nm thick GaP layer hosts the flatband metasurface, suspended with support structures over the silicon substrate (see Figure 2). To allow for the maximal range of band tuning by adjusting the fill factor, an optimal partial etch depth of 182 nm was selected so that a fill factor of 50% resulted in the desired flat band. The chosen period, a, was 436 nm and the period-doubling asymmetry, α, was .1.

The suspended flatband metasurfaces were fabricated by using a 210 nm thick GaP membrane on silicon from the commercial vendor NAsP III/V GmbH grown via chemical vapor deposition (CVD). A piece of the wafer was spin-coated with 400 nm of Zeon ZEP520A resist and then patterned using a 100 kV JEOL JBX6300FX electron-beam lithography tool to create the mask. The chip was then etched in a reactive ion etcher (RIE) using Cl_2/Ar chemistry. Partial etching was performed at an estimated rate of 4 nm/s and total etch time was calibrated through etch-tests to target the optimal partial etch depth of 182 nm. A second electron-beam step patterned the ZEP resist to make a mask for etching trenches down to the silicon substrate, and the pattern was again transferred to the GaP film using RIE. Finally, the silicon underneath the GaP membrane was removed using vapor phase xenon difluoride (XeF_2) which delivers a stiction-free and residue-free etching.

MEASUREMENT OF THE BAND STRUCTURE

We probed the fabricated metasurfaces via energy-momentum (E-K) spectroscopy, employing a spectrometer in combination with a Fourier lens relay to directly image the angle-resolved emission of a sample. A 4f relay was used to image the back focal plane of the objective onto the entrance slit of the spectrometer (Figure 3a). The image of the back focal plane was aligned to the spectrometer slit so that only emission along the y-axis of the metasurface was collected in the spectrometer. The objective used had a numerical aperture of 0.95, equivalent to greater than 70° of half angle. This wide angular range allows for the identification and resolution of the angular

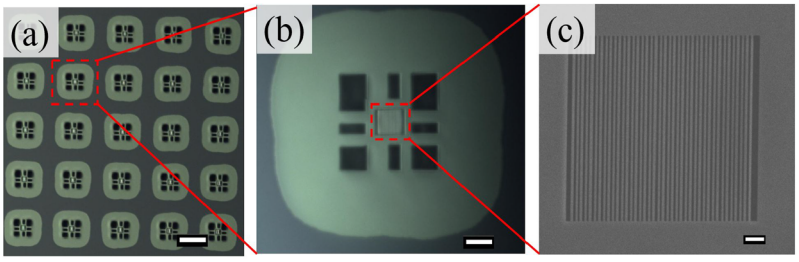

Figure 2. (a) Optical microscope image of an array of fabricated metasurfaces; scale bar 50 μm. The halo around each structure comes from the membrane being floating. (b) Optical microscope image of an individual flatband metasurface; scale bar 10 μm. (c) Scanning electron microscope image of the metasurface structures; scale bar 1 μm.

https://doi.org/10.1021/acsphotonics.3c00175
ACS Photonics XXXX, XXX, XXX−XXX

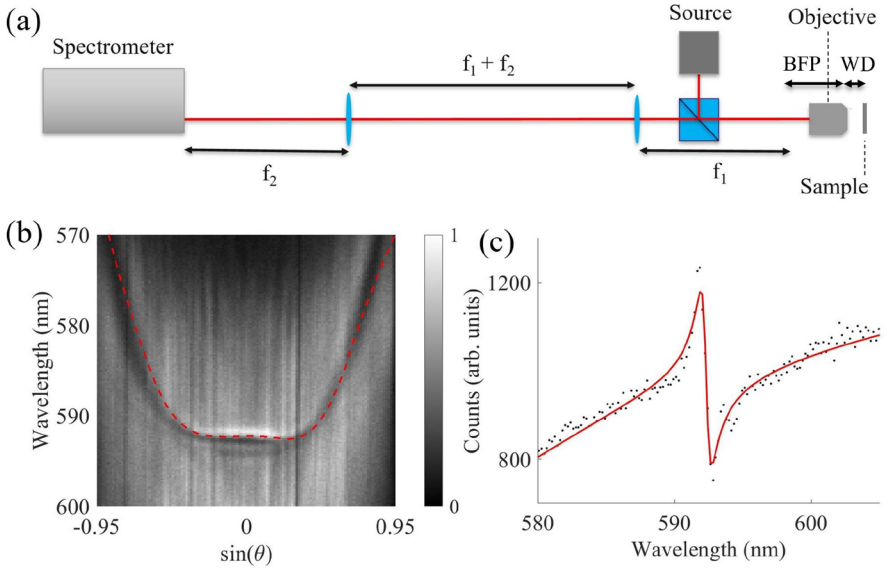

Figure 3. (a) Schematic of the energy-momentum spectroscopy setup. Working distance of the objective, WD = 0.35 mm, back focal distance, BFP = 8 mm, and lenses to image the back focal plane onto the spectrometer with focal distances f_1 = 75 mm, and f_2 = 150 mm. (b) Measured band structure of the flatband device: red-dashed line shows the resonance frequencies obtained via fitting a Fano resonance to the spectrum at each angle of reflection. We clearly observe a flatband dispersion. (c) Spectrum of the flatband resonance at the Γ-point ($\theta = 0$) in reflection normal to the plane of the metasurface; red line shows the fit of a Fano line shape to the resonance.

span of the designed flatband. For reflection measurements, illumination was provided by collimated fiber-coupled broadband light from a stabilized tungsten-halogen source (Thorlabs SLS301). The properties of the flatband were extracted directly from this measurement by fitting to determine the quality factor and angular extent of the flatband.

The interference between transmitted light and the resonant band of the metasurface results in a Fano line shape when the spectrum of the band is measured at each emission angle. Fitting a Fano resonance to each spectrum, we extract the resonant wavelength and quality factor for the flat band at each angle of emission along the *y*-axis of the metasurface (Figure 3b). At the Γ-point ($\theta = 0$) of the photonic band structure, the quality factor is measured to be ∼750, across a flatband range of 10° of half angle (see Figure 3c). Compared to a simulated quality factor of ∼1300, obtained via fitting with a Fano resonance, we found a reduced quality factor in the experiment most likely due to fabrication imperfections. Investigation of fabrication robustness and random fabrication error in similar metasurface devices has shown similar decrease in quality factor due to randomly distributed fabrication errors.[16] Thus, while creation of an array of devices has avoided perturbation of the flatband by correcting for systemic error in etch rate, variation of elements within a given device may inevitably affect the desired quality factor of the flatband resonance.

Creation of a flatband is one main application for dispersion engineering, but alternate band shapes have shown promise for realizing novel polaritonic interactions[17] or symmetry-breaking bound states in the continuum.[18] As a product of our fabricated array of metasurfaces with different fill factors, we also realized the bending of a flatband into a near flatband and a multivalley W-band dispersion (see Figure 4). These multivalley states have been explored as platforms for valley-polariton systems and exotic phenomena in Bose−Einstein condensates.[19]

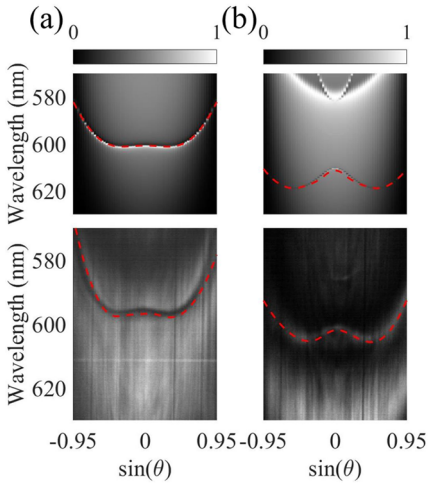

Figure 4. (a) Measured and simulated near flatband as fill factor is increased and the band bends away from a flatband; red-dashed lines indicate a fit of Fano resonances for each angle of emission. (b) Measured and simulated multivalley W-band dispersion as fill factor is increased even more with resonances shown by red-dashed lines.

INTEGRATION WITH CDSE NPLS

While identification of the visible flatband in reflection validates the metasurface design, to establish the utility of enhancing light−matter interaction, near-field coupling to material is desired. CdSe NPLs, quasi two-dimensional nanocrystals with quantum confined excitons, are particularly promising as emitters due to their narrow inhomogeneous line width and ease of integration as a colloidal suspension. Researchers have already shown room temperature strong coupling of NPLs with arrays of plasmonic holes.[20,21] By controlling the number of monolayers in an NPL, the emission wavelength can be precisely tuned, making them attractive for light emitting devices and polaritonics.[22,23] Specifically, six monolayer thick CdSe NPLs have a sharp excitonic resonance

https://doi.org/10.1021/acsphotonics.3c00175
ACS Photonics XXXX, XXX, XXX−XXX

at 585 nm, just off resonance to the photonic flatband. The 6-monolayer (1.9 nm) thick zinc-blende CdSe nanoplatelets were grown using a direct synthesis method reported by Cho et al.[24] and dispersed in methyl cyclohexane or toluene. Detailed synthesis and characterization can be found in the Supporting Information. By dropcasting a CdSe NPL solution on the metasurface, we integrated the emitters without straining the mechanically fragile floating membrane.

Once integrated, the emission of NPL PL into the flatband mode was verified with above-band excitation via a 532 nm laser and energy-momentum spectroscopy. While a randomly oriented collection of NPLs will show isotropic emission at its resonant wavelength, emission into the photonic flatband showed enhanced PL outside of the main excitonic peak. We realized both of these features experimentally, showing the standard NPL PL centered on 587 nm and flatband-enhanced PL near 597 nm (see Figure 5a). Unlike a photonic crystal

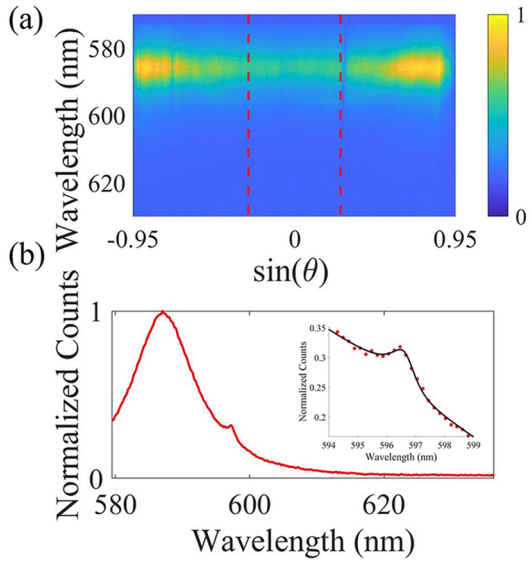

Figure 5. (a) Measured PL from NPLs coupled to a GaP metasurface showing standard PL extending across all angles of emission as well as the photonic flatband mode enhancing PL. Red dashed lines highlight the angular extent of the flatband. (b) Integrated PL over the flatband as bounded by red dashed line in (a) showing the main NPL PL peak and the smaller peak due to coupling with the GaP measurface. Inset: the flatband PL peak fit with as a Fano resonance, resulting in a measured quality factor of $Q \sim 550$.

defect resonator or traditional grating, the enhancement is not limited to a single location or angle of emission. However, the ease of integration with our metasurface for dispersion engineering also led to an overabundance of colloidal material uncoupled with the cavity mode, as seen in the dominance of the spectrum by the background, uncoupled NPL emission. Application of masking or patterning techniques for material deposition and activation may be explored to enhance the coupled PL relative to the background. Additionally, future design for a stronger field on the surface and within air above the metasurface can potentially provide stronger coupling with the emitters. Integration of the PL spectrum over the angles of emission in the flatband shows the main PL peak as well as the enhanced flatband emission (see Figure 5b) with subsequent fitting with a Fano Resonance resulting in a calculated quality factor, $Q > 500$. Thus, our GaP flatband metasurface demonstrates a platform for highly selectively enhancing the PL of emitters at a given visible wavelength while maintaining emission over a wide range of angles.

CONCLUSION

Our demonstrated visible flatband metasurface represents a step toward future optical applications of engineering dispersion and light−matter interaction. A flatband metasurface in the visible regime creates possibilities in engineering light−matter interactions with emerging quantum emitters. Flatband coupled PL from CdSe NPLs illustrates one such example. Transitioning our design to mechanically stable on-substrate platforms will potentially allow for more extensive material integration. Increasing quality factor, for example, by reducing the period-doubling asymmetry parameter, or selection of another visible wavlength emitter may allow for potential room temperature strong coupling or the creation of degenerate polariton states. Photonic moiré devices have recently shown potential to expand the angular reach of flatbands.[25] Looking forward, expansion of flatband modes to encompass all of the *k*-space may lead to free-space-integrated slow light metasurfaces.

ASSOCIATED CONTENT

Supporting Information

The Supporting Information is available free of charge at https://pubs.acs.org/doi/10.1021/acsphotonics.3c00175.

Fabrication procedure for CdSe NPL and discussion of fano resonance fitting (PDF)

AUTHOR INFORMATION

Corresponding Author

Arka Majumdar − *Department of Physics, University of Washington, Seattle, Washington 98195, United States; Electrical and Computer Engineering, University of Washington, Seattle, Washington 98195, United States;* orcid.org/0000-0003-0917-590X; Email: arka@uw.edu

Authors

Christopher Munley − *Department of Physics, University of Washington, Seattle, Washington 98195, United States;* orcid.org/0000-0001-5684-3144

Arnab Manna − *Department of Physics, University of Washington, Seattle, Washington 98195, United States;* orcid.org/0009-0007-0056-9650

David Sharp − *Department of Physics, University of Washington, Seattle, Washington 98195, United States;* orcid.org/0000-0002-1034-8567

Minho Choi − *Electrical and Computer Engineering, University of Washington, Seattle, Washington 98195, United States*

Hao A. Nguyen − *Department of Chemistry, University of Washington, Seattle, Washington 98195, United States;* orcid.org/0000-0001-6742-1748

Brandi M. Cossairt − *Department of Chemistry, University of Washington, Seattle, Washington 98195, United States;* orcid.org/0000-0002-9891-3259

Mo Li − *Department of Physics, University of Washington, Seattle, Washington 98195, United States; Electrical and Computer Engineering, University of Washington, Seattle, Washington 98195, United States;* orcid.org/0000-0002-5500-0900

https://doi.org/10.1021/acsphotonics.3c00175
ACS Photonics XXXX, XXX, XXX−XXX

Arthur W. Barnard − *Department of Physics, University of Washington, Seattle, Washington 98195, United States; Materials Science & Engineering, University of Washington, Seattle, Washington 98195, United States*

Complete contact information is available at: https://pubs.acs.org/10.1021/acsphotonics.3c00175

Notes

The authors declare no competing financial interest.

■ ACKNOWLEDGMENTS

We thank Lorryn Wilhelm for assistance with figure development.This material is based upon work supported by the National Science Foundation. grant no. DMR-2019444. Part of this work was conducted at the Washington Nanofabrication Facility/Molecular Analysis Facility, a National Nanotechnology Coordinated Infrastructure (NNCI) site at the University of Washington with partial support from the National Science Foundation via awards NNCI-1542101 and NNCI-2025489.

■ REFERENCES

(1) Tang, L.; Song, D.; Xia, S.; Xia, S.; Ma, J.; Yan, W.; Hu, Y.; Xu, J.; Leykam, D.; Chen, Z. Photonic Flat-Band Lattices and Unconventional Light Localization. *Nanophotonics* **2020**, *9* (5), 1161−1176.

(2) Mukherjee, S.; Spracklen, A.; Choudhury, D.; Goldman, N.; Öhberg, P.; Andersson, E.; Thomson, R. R. Observation of a Localized Flat-Band State in a Photonic Lieb Lattice. *Phys. Rev. Lett.* **2015**, *114* (24), 245504.

(3) Jacqmin, T.; Carusotto, I.; Sagnes, I.; Abbarchi, M.; Solnyshkov, D. D.; Malpuech, G.; Galopin, E.; Lemaître, A.; Bloch, J.; Amo, A. Direct Observation of Dirac Cones and a Flatband in a Honeycomb Lattice for Polaritons. *Phys. Rev. Lett.* **2014**, *112* (11), 116402.

(4) Baboux, F.; Ge, L.; Jacqmin, T.; Biondi, M.; Galopin, E.; Lemaître, A.; Le Gratiet, L.; Sagnes, I.; Schmidt, S.; Türeci, H. E.; Amo, A.; Bloch, J. Bosonic Condensation and Disorder-Induced Localization in a Flat Band. *Phys. Rev. Lett.* **2016**, *116* (6), 066402.

(5) Xu, C.; Wang, G.; Hang, Z. H.; Luo, J.; Chan, C. T.; Lai, Y. Design of Full-k-Space Flat Bands in Photonic Crystals beyond the Tight-Binding Picture. *Sci. Rep.* **2015**, *5* (1), 18181.

(6) Nakata, Y.; Okada, T.; Nakanishi, T.; Kitano, M. Observation of Flat Band for Terahertz Spoof Plasmons in a Metallic Kagomé Lattice. *Phys. Rev. B* **2012**, *85* (20), 205128.

(7) Cueff, S.; Dubois, F.; Huang, M. S. R.; Li, D.; Zia, R.; Letartre, X.; Viktorovitch, P.; Nguyen, H. S. Tailoring the Local Density of Optical States and Directionality of Light Emission by Symmetry Breaking. *IEEE Journal of Selected Topics in Quantum Electronics* **2019**, *25* (3), 1−7.

(8) Melli, M.; West, M.; Hickman, S.; Dhuey, S.; Lin, D.; Khorasaninejad, M.; Chang, C.; Jolly, S.; Tae, H.; Poliakov, E.; St. Hilaire, P.; Cabrini, S.; Peroz, C.; Klug, M. Gallium Phosphide Optical Metasurfaces for Visible Light Applications. *Sci Rep* **2020**, *10* (1), 20694.

(9) Wu, S.; Buckley, S.; Schaibley, J. R.; Feng, L.; Yan, J.; Mandrus, D. G.; Hatami, F.; Yao, W.; Vučković, J.; Majumdar, A.; Xu, X. Monolayer Semiconductor Nanocavity Lasers with Ultralow Thresholds. *Nature* **2015**, *520* (7545), 69−72.

(10) Rivoire, K.; Kinkhabwala, A.; Hatami, F.; Masselink, W. T.; Avlasevich, Y.; Müllen, K.; Moerner, W. E.; Vučković, J. Lithographic Positioning of Fluorescent Molecules on High-Q Photonic Crystal Cavities. *Appl. Phys. Lett.* **2009**, *95* (12), 123113.

(11) Liu, V.; Fan, S. S4: A Free Electromagnetic Solver for Layered Periodic Structures. *Comput. Phys. Commun.* **2012**, *183* (10), 2233−2244.

(12) Zeng, B.; Majumdar, A.; Wang, F. Tunable Dark Modes in One-Dimensional "Diatomic" Dielectric Gratings. *Opt. Express, OE* **2015**, *23* (10), 12478−12487.

(13) Nguyen, H. S.; Dubois, F.; Deschamps, T.; Cueff, S.; Pardon, A.; Leclercq, J.-L.; Seassal, C.; Letartre, X.; Viktorovitch, P. Symmetry Breaking in Photonic Crystals: On-Demand Dispersion from Flatband to Dirac Cones. *Phys. Rev. Lett.* **2018**, *120* (6), 066102.

(14) Overvig, A. C.; Shrestha, S.; Yu, N. Dimerized High Contrast Gratings. *Nanophotonics* **2018**, *7* (6), 1157−1168.

(15) Leykam, D.; Flach, S. Perspective: Photonic Flatbands. *APL Photonics* **2018**, *3* (7), 070901.

(16) Kühne, J.; Wang, J.; Weber, T.; Kühner, L.; Maier, S. A.; Tittl, A. Fabrication Robustness in BIC Metasurfaces. *Nanophotonics* **2021**, *10* (17), 4305−4312.

(17) Pickup, L.; Sigurdsson, H.; Ruostekoski, J.; Lagoudakis, P. G. Synthetic Band-Structure Engineering in Polariton Crystals with Non-Hermitian Topological Phases. *Nat Commun* **2020**, *11* (1), 4431.

(18) Mermet-Lyaudoz, R.; Dubois, F.; Hoang, N.-V.; Drouard, E.; Berguiga, L.; Seassal, C.; Letartre, X.; Viktorovitch, P.; Nguyen, H. S. Realization of Bound State In the Continuum Induced by Vertical Symmetry Breaking in Photonic Lattice. *arXiv* 2019, arXiv:1905.03868, DOI: 10.48550/arXiv.1905.03868.

(19) Sun, M.; Savenko, I. G.; Flayac, H.; Liew, T. C. H. Multivalley Engineering in Semiconductor Microcavities. *Sci Rep* **2017**, *7* (1), 45243.

(20) Pelton, M. Carrier Dynamics, Optical Gain, and Lasing with Colloidal Quantum Wells. *J. Phys. Chem. C* **2018**, *122* (20), 10659−10674.

(21) Winkler, J. M.; Rabouw, F. T.; Rossinelli, A. A.; Jayanti, S. V.; McPeak, K. M.; Kim, D. K.; le Feber, B.; Prins, F.; Norris, D. J. Room-Temperature Strong Coupling of CdSe Nanoplatelets and Plasmonic Hole Arrays. *Nano Lett.* **2019**, *19* (1), 108−115.

(22) Qu, J.; Rastogi, P.; Gréboval, C.; Livache, C.; Dufour, M.; Chu, A.; Chee, S.-S.; Ramade, J.; Xu, X. Z.; Ithurria, S.; Lhuillier, E. Nanoplatelet-Based Light-Emitting Diode and Its Use in All-Nanocrystal LiFi-like Communication. *ACS Appl. Mater. Interfaces* **2020**, *12* (19), 22058−22065.

(23) Qiu, L.; Mandal, A.; Morshed, O.; Meidenbauer, M. T.; Girten, W.; Huo, P.; Vamivakas, A. N.; Krauss, T. D. Molecular Polaritons Generated from Strong Coupling between CdSe Nanoplatelets and a Dielectric Optical Cavity. *J. Phys. Chem. Lett.* **2021**, *12* (20), 5030−5038.

(24) Cho, W.; Kim, S.; Coropceanu, I.; Srivastava, V.; Diroll, B. T.; Hazarika, A.; Fedin, I.; Galli, G.; Schaller, R. D.; Talapin, D. V. Direct Synthesis of Six-Monolayer (1.9 Nm) Thick Zinc-Blende CdSe Nanoplatelets Emitting at 585 Nm. *Chem. Mater.* **2018**, *30* (20), 6957−6960.

(25) Nguyen, D. X.; Letartre, X.; Drouard, E.; Viktorovitch, P.; Nguyen, H. C.; Nguyen, H. S. Magic Configurations in Moiré Superlattice of Bilayer Photonic Crystals: Almost-Perfect Flatbands and Unconventional Localization. *Phys. Rev. Res.* **2022**, *4* (3), L032031.